Studies of the Cerenkov emission angle reconstruction. Part 1

P. Schiavon

COMPASS / RICH / PS / Report 2.b

10/ 6/97 - rev. 7/11/97.

1 Note :

The reconstruction method described is characterized by the fact that, for each detected photon, the emission angle is computed assuming that the photon has been emitted from the centre of the particle path inside the radiator; the average of all the reconstructed values is taken as the measured angle.
See, e.g., T. Ypsilantis and J. Seguinot, Nucl. Instr. and Methods, A343 (1994) 30.

2 Assumptions :

a) The origin of the reference system is in the nominal centre of the mirror;
coordinates: x_c, y_c, z_c;
the z-axis is parallel to the beam line, the y-axis vertical and the x-axis horizontal to the left (looking downstream).

b) The detector is defined as a plane surface on which the impact point of each photon is measured with some resolution (e.g.: $8.mm \times 8.mm$ pixel);
coordinates: x_{de}, y_{de}, z_{de}.

c) The particle trajectory is assumed to be (well) measured both in angle and position by external independent detectors.

d) The Cerenkov photons are emitted with an uniform distribution in distance (s) along the particle path length inside the radiator and in angle (ϕ) around the particle trajectory, but the emission point is not known;
the best estimate of such an emission point is the 'average', i.e. the middle point of the particle path inside the radiator; it will be the same for all the photons emitted by the same particle;
coordinates: x_{ph}, y_{ph}, z_{ph}.

3 Procedure :

a) Each photon emitted impinges on the mirror and then is reflected to the detector surface;
the normal to the mirror at the photon impact point points to the reference system origin (it coincides with the mirror centre);
by the Snell law, incident ray, normal to the reflecting surface and reflected ray are coplanar; it follows that the photon emission point, the reflection point on the mirror, the detection point on the detector and the mirror centre lie on the same plane (photon plane).

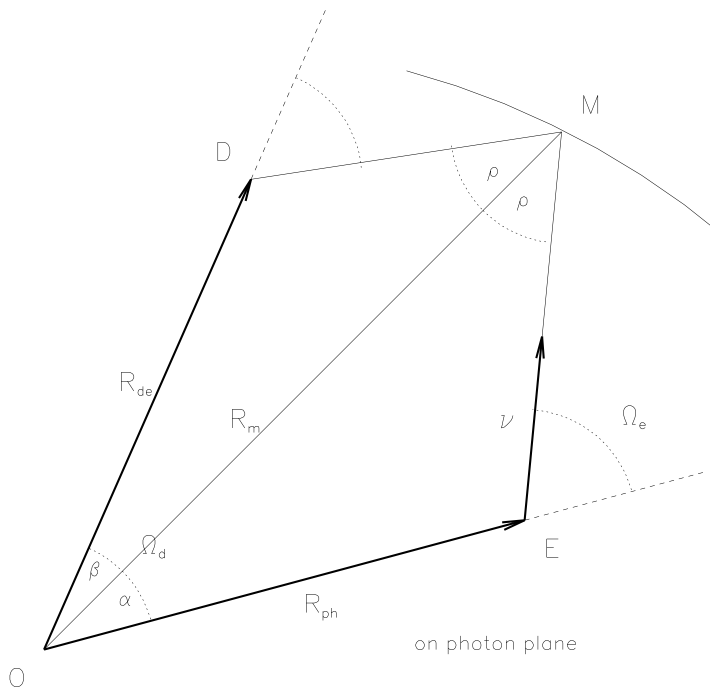

Figure 1: Geometry of the reconstruction.

b) On the photon plane (fig. 1) :
$R_{de} = \sqrt{x_{de}^2 + y_{de}^2 + z_{de}^2}$ is the length of the vector $\bar{R}_{de}$ defining the photon detection point,
$R_{ph} = \sqrt{x_{ph}^2 + y_{ph}^2 + z_{ph}^2}$ is the length of the vector $\bar{R}_{ph}$ defining the photon 'emission' (middle) point,
Ω_d is the angle between the vectors $\bar{R}_{de}$ and $\bar{R}_{ph}$ (known),
Ω_e is the angle between the vector $\bar{R}_{ph}$ and the emitted photon direction $\bar{\nu}$,
ρ is the photon incidence and reflection angle on the mirror,
R_m is the mirror nominal radius;
the goal is the reconstruction of the emitted photon direction $\bar{\nu}$.

c) Let O be the origin, D the detection point, E the emission point and M the reflection point (on the photon plane); with reference to the triangle OEM , we write :

$$\frac{\sin(\rho + \alpha)}{R_m} = \frac{\sin\rho}{R_{ph}} = \frac{\sin\Omega_e}{R_m} \tag{1}$$

where α is the angle in O; with reference to the triangle ODM we write :

$$\frac{\sin(\rho+\beta)}{R_m} = \frac{\sin\rho}{R_{de}} \tag{2}$$

where β is the angle in O ; combining (1) and (2) :

$$\sin(\rho+\beta) = \frac{R_{ph}\sin\Omega_e}{R_{de}}; \tag{3}$$

with reference to the quadrilateral OEMD :

$$\Omega_e = \Omega_d - corr \qquad\qquad corr = (\rho+\beta) - (2\rho) \tag{4}$$

and from (3), (1) and (4) :

$$corr = \arcsin\left(\frac{R_{ph}\sin\Omega_e}{R_{de}}\right) - 2\arcsin\left(\frac{R_{ph}\sin\Omega_e}{R_m}\right) \tag{5}$$

d) The solution of (4) for Ω_e is not straightforward; but, because *corr* is small compared to Ω_d and Ω_e, we can use an iterative procedure, assuming at the first pass $\Omega_e = \Omega_d$ in the (5) and then using Ω_e from (4) into (5);
typically three iterations are enought.

e) In the photon plane, the emitted photon direction (unit) vector $\bar{\nu}$ can be expressed as a linear combination of the position vectors $\bar{R}_{de}$ and $\bar{R}_{ph}$ (fig. 2) :

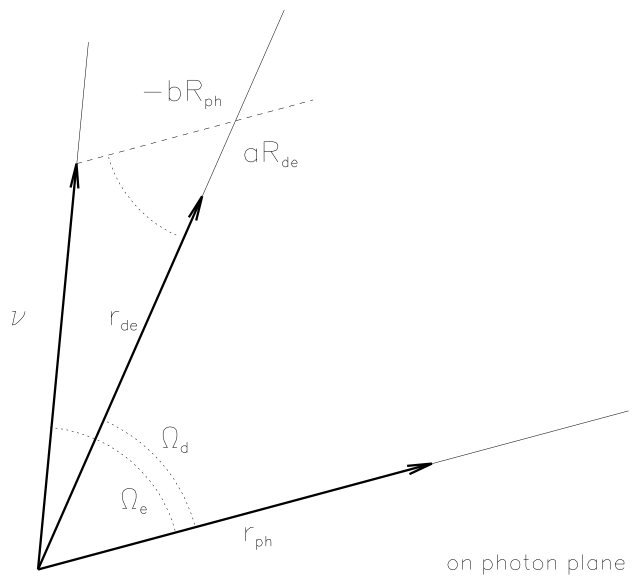

Figure 2: Geometry of the reconstruction.

$$\bar{\nu} = a\bar{R}_{de} + b\bar{R}_{ph}$$

note that Ω_d is the angle between $\bar{R}_{de}$ and $\bar{R}_{ph}$ and that Ω_e is the angle between $\bar{\nu}$ and $\bar{R}_{ph}$; then, applying twice the sine theorem :

$$\sin \Omega_d = \frac{\sin \Omega_e}{a}$$
$$\sin \Omega_d = \frac{\sin (\Omega_e - \Omega_d)}{b}$$
$$\bar{\nu} = \frac{\sin \Omega_e}{\sin \Omega_d} \bar{R}_{de} - \frac{\sin (\Omega_e - \Omega_d)}{\sin \Omega_d} \bar{R}_{ph} \qquad (6)$$

f) The photon emission angle θ_C can then be computed from the direction of $\bar{\nu}$ and that of the particle ($\bar{P}$).

$$\theta_C = \arccos \left(\frac{\bar{\nu} \cdot \bar{P}}{P} \right)$$

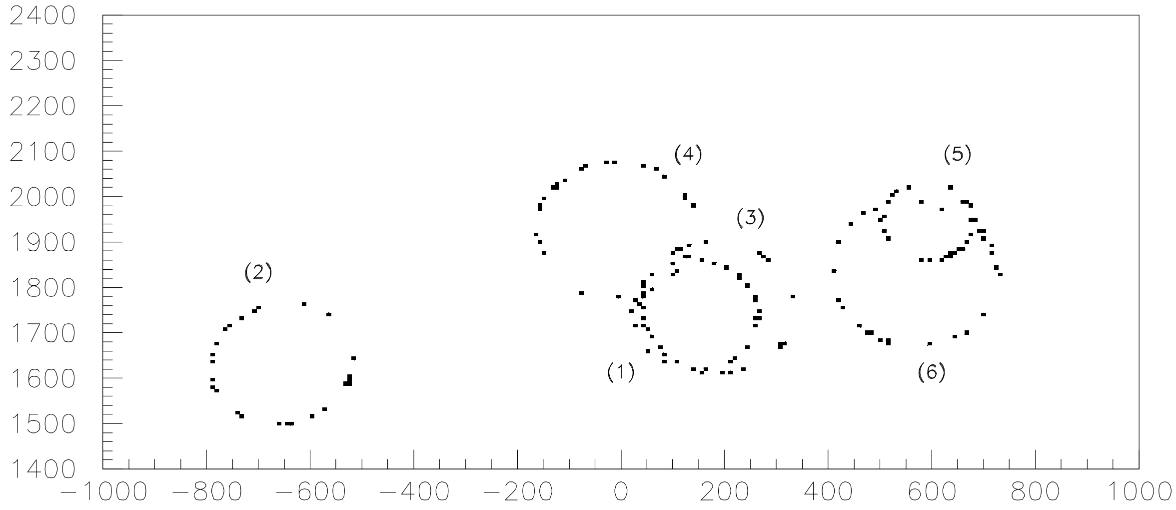

Figure 3: Simulated event with six particles of different β : distribution of the active pixels on the detector.

4 Hints for the pattern recognition:

a) For 'pattern recognition' I mean a procedure to select the photon hits on the detector due to the photons emitted by a single particle among all the others.
the most relevant feature of the RICH is that the photon hits distribute along the 'ring' (more or less a circumference) on the detector surface and this fact is the basis of many pattern recognition methods used.

b) In the present simulation a very simple recipe has been used to introduce the finite resolution of the photon detector; the detector surface is divided into square pixels ($8.mm \times 8.mm$) and, for the photons hitting the pixel surface, its centre is assumed as hit position, counting it as many times as the photons hitting it. No clustering has been taken into account.
In an event with many particles producing Cerenkov photons, the detector surface is covered by the corresponding rings, mostly intersecting, with different radii, and by some 'background' hits; I will make no hypothesis on the distribution and the characteristics

	physical distribution	uniform distribution
	σ_θ μrad	σ_θ μrad
spherical aberration	95.	80.
spherical aberr. and pixel	172.	167.

Table 1: Resolution in reconstructed Cerenkov angle θ_C (RICH 1). In row 1 only spherical aberrations are taken into account; in row 2 the detector resolution is included, using the pattern recognition procedure described in point 4.

of the background.

c) A particular pattern recognition procedure is directely associated to the reconstruction method described above.
Assuming, as stressed above, that the particle trajectories are measured, for each one of them, the emission angles are reconstructed for all the photons detected as they were all emitted by that particle; in a plot ϕ vs θ (θ and ϕ polar emission angles around the particle trajectory) the photons really emitted by that particle cluster along a straight line at fixed θ and full range (0. to 2π) in ϕ (at least in the case of full acceptance for the photons); the 'pattern' to be looked for reduces to a straight line, which, at least in principle, can be recognized in a easier way.

d) In fig.3 a typical simulated event with 6 particles of different β is shown; the six rings, with different radii, intersect each other, but no background is taken into account. In fig.4 (a) to (c) and (g) to (i), the ϕ vs θ plots for the particle indicated are shown, together with the corresponding projections on the θ axis (fig.4 (d) to (f) and (j) to (l)) where the peak of the 'good' photons is quite evident in all the cases.
It is obvious that the background will complicate the picture. On the other hand some filter can be envisaged to reduce the number of photons that have to be reconstructed for each particle. Moreover, the problem of double (or more) counting of the photons, due to the fact that some rings are crossing each other, which distorts the resolution of the Cerenkov emission angle measurement for a ring, needs, as in most of the other different approaches to the ring pattern recognition, to be solved separately.

5 Results :

In the simulation we have used a sample of particles from a file of LEPTO generated events as described in COMPASS / RICH / PS / Report 1, with a θ_C distribution peaked at rather high values; moreover, for comparison, data are also available from a sample of particles with θ_C uniformely distributed between 10. and 60. $mrad$ ($\beta = 1.$ corresponds to $\theta_C = 55.8$ $mrad$ in the case of RICH 1).

We obtain the results shown in table 1.
To evaluate the *ring* resolution in θ_C, a fixed number of 30 photons per particle has been simulated (first row of the table).
To evaluate the effects of the experimental resolution of the detector, the pattern recognition procedure proposed at point 4 above has been used (second row of the table).

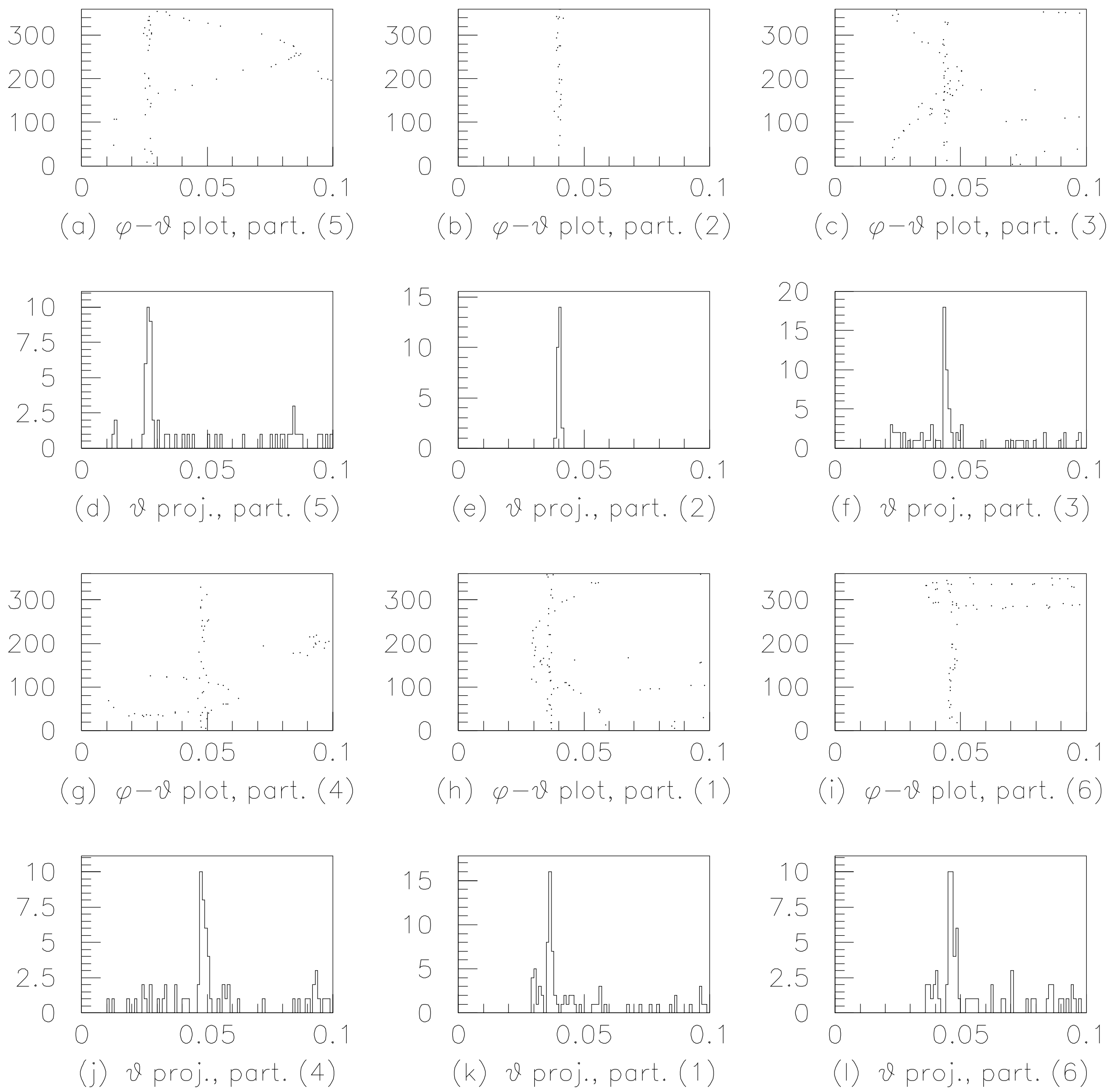

Figure 4: Pattern recognition of the 'rings' of the six particles.